Available online at www.sciencedirect.com
SCIENCE DIRECT®
Materials Science in Semiconductor Processing 8 (2005) 587–601
MATERIALS SCIENCE IN SEMICONDUCTOR PROCESSING

Molecular dynamics study of copper trench filling in damascene process

R.T. Hong[a], M.J. Huang[a], J.Y. Yang[b,*]

[a]*Department of Mechanical Engineering, National Taiwan University, Taipei 10764, Taiwan*
[b]*Institute of Applied Mechanics, National Taiwan University, Taipei 10764, Taiwan*

Available online 2 August 2005

Abstract

The trench filling of depositing copper atoms on the titanium layer in a damascene process was studied using molecular dynamics simulation with the embedded atom method (EAM) as interaction potential for the present alloy metal system. A three-layer trench model consisting of the barrier, thermal control, and fixed layers was used. The effects of different process parameters on the trench-filling morphologies and microstructures including incident energies of depositing atoms and substrate temperatures were investigated. The present results using invariance-preserving alloy model are discussed in terms of void formation, coverage percentage, and alloy fraction and compared with simple arithmetic average alloy model.

Keywords: Molecular dynamics simulation; Embedded atom method; Damascene process

1. Introduction

The formation of metal interconnects is a key aspect of the modern semiconductor integrated circuits manufacturing. As feature sizes decrease below a quarter micron, the scaling of interconnects poses several serious metallization problems. Copper is the clear choice at technology of 0.18 μm and smaller because it provides speed enhancement with no sacrifice of device reliability. The advantage of copper is that it has better RC delay time, which means metal connect layer is increasing as well as the distance between wires is shorter and shorter. The copper process is entirely different from that of aluminum. Aluminum is typically blanket deposited and etched, followed by the deposition of an insulating dielectric. Copper, on the other hand, is patterned in a way called damascene processing. The damascene technology [1] using copper chemical mechanical polishing is the main solution known to be able to pattern copper with a large process window. In a damascene process, trenches or vias are first etched in a flat dielectric and then a conducting metal is placed in the cavities. Previously, aluminum and its alloys had been the most commonly used materials for conductor. However, for future electronic applications, those materials cannot be used as they are vulnerable to electromigration (EM) and have rather high resistance. The major EM failure mechanism depends on the diffusion process and both the values of activation energy and melting temperature of Cu are higher than that of Al, thus Cu has lower mobilities for self-diffusion [2]. The electromigration resistance has been demonstrated experimentally that Cu interconnects have on the order of 10x to 100x better than Al interconnects [3]. To improve the electrical properties, copper is used as a metallic material alternative to aluminum for modern

*Corresponding author. Present Address: No. 1, Section 4, Roosevelt Road, Taipei, Taiwan.
E-mail address: yangjy@spring.iam.ntu.edu.tw (J.Y. Yang).

1369-8001/$ - see front matter © 2005 Elsevier Ltd. All rights reserved.
doi:10.1016/j.mssp.2005.05.001

semiconductor industry. The disadvantage of copper is due to its difficulty to adhesive on dielectric materials (SiO_2, etc.) and the copper atoms will penetrate into dielectric materials. To prevent the metal from diffusing into dielectric materials, a thin layer on the inner surface of the pattern dielectric is required and an additional thin layer to prompt the adhesion of copper on dielectric layer. This layer is called barrier layer. The materials of barrier layer used include titanium (Ti), titanium nitride (TiN), and various refractory metals and compounds. With the insertion of a Ti layer, the wetting property of the Cu improves and the EM lifetime of Cu damascene interconnects is significantly longer than that for interconnects without inserted Ti layer. On the manufacturing aspect, the deposition methods including physical vapor deposition (PVD), chemical vapor deposition (CVD), and electroplating are dominant. For microelectronic devices, film layers are often grown on top of another, with different materials used to produce conduction and passive layers. In such applications, feature geometries such as steps, trenches, and contact holes are used to form interconnects between layers. Deposition film coverage along both vertical and horizontal edges of nonplanar features is required for proper device operation. As the density of nonplanar surface features becomes higher, the feature sizes are getting smaller, making uniform coverage more difficult. In general, sputter deposition into these features may result in overhang and eventually void formation, which causes resistance increase and reliability concerns. In addition, various process parameters including incident energy, substrate temperature, deposition rate, flux distribution, and trench geometry can affect the morphology and microstructure of the features. In deposition simulation, many simulation approaches have been explored for this class of problems. They can be roughly divided into two categories; continuum-based methods and atomistic model methods. The continuum approach seeks to present the surface as described by an equation with mesh points embedded in the system such as shock-tracking algorithm of Hamaguchi and Rossnagel [4] and Adalsteinsson and Sethian [5]. Most atomistic models are based on Monte Carlo (MC) method [6,7] and molecular dynamics (MD) simulation [8]. *A recent study on the sputter deposition trench filling in Damascene process using MD with pair-wise potential has been given in* [9]. The MD can provide a valuable tool for revealing the detailed mechanism and microstructures during the deposition process. The characteristic length of interconnect will approach sub-micron region which is comparable to the diffusion length of other methods for this problem, that makes atomistic method the suitable one for the process. In this work, we investigate the trench-filling behavior of depositing copper atoms onto the titanium diffusion barrier layer in a damascene process using MD simulation. First, we study the effects of different process parameters including incident energies of depositing atoms and substrate temperatures on the trench-filling microstructures. Next, we also examine the effect due to the difference of invariance-preserving alloy two-body potential model and simple arithmetic average model. For the interatomic potential between different metals, Johnson's invariance-preserving embedded atom method (EAM) is used. For manipulating the interatomic potential between different metal atoms, the simple average had been used in most MD computations in previous works. We examine the differences of these two alloy models. The rest of the paper is organized as follows. In Section 2, the basic embedded atom method and its alloy model are briefly described. The trench model and molecular dynamics simulation technique used are outlined in Section 3. In Section 4, the simulated results are presented for several process parameters and their effects on the trench-filling morphologies are discussed. Finally, some concluding remarks are given in Section 5.

2. Embedded atom method potentials

In many metallic systems, interatomic potentials developed based on the EAM are in good agreement with experimental result. EAM is an isotropic many-body pair-function potential. This section is divided into two parts. First, we describe the basic EAM and second the alloy model with EAM. Stott and Zaremba [10] have shown that the energy of a host containing an impurity is a function of the electron density of the unperturbed host, i.e., the host with the impurity absent. The EAM, originally developed by Daw and Baskes [11], was derived based on density functional theory (DFT). The electron density at each particle position is determined as superposition from surrounding atoms. The embedding energy, i.e., the energy required to place an atom in an electron gas, is then determined as a function of the local electron density. It provides a practical method to account for the effect of the local environment on the interaction between atoms, thus, providing more realistic force values. The EAM is obtained by empirically fitting the prediction of potential to measured materials [12]. A nearest neighbor EAM potential in a simple analytic form that is well suited to MD simulations has been proposed by Johnson [13] and is adopted in this work. The analytical forms of EAM have been developed for many metals and have yielded reasonable fits to physical properties [14]. The total energy acting on each atom is computed from the sum of the local embedded energy and two-body potential as

$$E_{\mathrm{tot}} = \sum_i F(\rho_i) + \frac{1}{2}\sum_i \sum_{j\neq i} \phi_{ij}(r_{ij}), \tag{1}$$

$$\rho_i = \sum_{j \neq i} f(r_{ij}), \tag{2}$$

where E_{tot} is the total internal energy, ρ_i is the local electron density at atom i due to all the other atoms, $\phi(r_{ij})$ is the pair potential and r_{ij} is the distance between atom i and atom j. The embedded energy, F, is the energy needed to embed the atom in the local-electron density as provided by the other atoms. This electron density is approximated by the superposition of atomic-electron density function, $f(r_{ij})$, which depends on the distance of neighbor atoms. The two-body potential and electron density function as given by Johnson can be written respectively as

$$\phi(r) = \frac{A e^{-\alpha(r/r_e - 1)}}{1 + (r/r_e - \kappa)^m} - \frac{B e^{-\beta(r/r_e - 1)}}{1 + (r/r_e - \lambda)^n}, \tag{3}$$

$$f(r) = \frac{f_e e^{-\beta(r/r_e - 1)}}{1 + (r/r_e - \lambda)^n}. \tag{4}$$

The pair potential model is a Morse-type potential which is composed of a short-range repulsive exponential and a long-range attractive exponential. The parameters in Eqs. (3)–(4) are given in Table 1. The embedding function models the attractive interaction as a function of the local electron density. The embedding energy of the atom i is determined by the local electron density at the position of the atom and the standard form of embedding function, F, is expressed as

$$F(\rho) = F_e \left(1 - \ln\left(\frac{\rho}{\rho_e}\right)^{\eta}\right)\left(\frac{\rho}{\rho_e}\right)^{\eta}, \tag{5}$$

where F_e is the embedding function evaluated at equilibrium electron density ρ_e. To yield smooth embedding functions that match appropriate physical criteria, Eq. (5) can be written as [15]

$$F(\rho) = \sum_{i=0}^{3} F_{ni}\left(\frac{\rho}{\rho_n} - 1\right)^i, \quad \rho < \rho_n, \ \rho_n = 0.85\rho_e, \tag{6}$$

$$F(\rho) = \sum_{i=0}^{3} F_i\left(\frac{\rho}{\rho_e} - 1\right)^i, \quad \rho_n \leqslant \rho < \rho_0, \ \rho_0 = 1.15\rho_e, \tag{7}$$

$$F(\rho) = F_0\left(1 - \ln\left(\frac{\rho}{\rho_e}\right)^{\eta}\right)\left(\frac{\rho}{\rho_e}\right)^{\eta}, \quad \rho_0 < \rho. \tag{8}$$

The parameters in Eqs. (6)–(8) are given in Table 2. Lastly, in order to use the potential in MD simulation we need to evaluate the forces as

$$\begin{aligned}\vec{F}_i &= -\nabla_{\vec{r}_i} E_{\text{tot}} \\ &= -\sum_{j \neq i}\left[\frac{\partial F_i(\rho_i)}{\partial \rho_i}\frac{\partial f_j(r_{ij})}{\partial r_{ij}} + \frac{\partial F_j(\rho_j)}{\partial \rho_j}\frac{\partial f_i(r_{ij})}{\partial r_{ij}} + \frac{\partial \phi_{ij}(r_{ij})}{\partial r_{ij}}\right]\frac{\vec{r}_i - \vec{r}_j}{r_{ij}}.\end{aligned} \tag{9}$$

For an alloy model with the EAM, an embedding function $F(\rho)$ and an atomic electron-density function $f(r)$ must be specified for each atomic species, and a two-body potential $\phi(r)$ specified for each possible combination of atomic species. Since the electron density at any location is taken as a linear superposition of atomic electron densities, and since the embedding energy is assumed to be independent of the source of the electron density, these two functions can be taken from monatomic models directly. For a binary alloy with a- and b-type atoms, ϕ^{aa} and ϕ^{bb} are given by the individual monatomic models, and ϕ^{ab} and ϕ^{ba} are assumed to be equal. A direct and simple possible form for the alloy potential can assume either the geometric or arithmetic average of two-body potential as has been tested by Foiles et al. [16]. However, a novel two-body alloy model with the same invariance to electron density transformations as fcc monatomic metal model has been constructed by Johnson [17]. In this work, we adopt Johnson's alloy model with EAM which satisfies the

Table 1
Electron density function and two-body potential parameters for metals of EAM

	r_e (Å)	f_e (eV/Å)	ρ_e (eV/Å)	α	β	A	B	κ	λ	m	n
Cu	2.556	1.554	22.150	7.670	4.091	0.328	0.469	0.431	0.863	20.0	20.0
Ti	2.930	1.860	25.600	8.780	4.680	0.328	0.469	0.431	0.863	20.0	20.0

Table 2
Embedding function parameters for metals of EAM

	η	F_{n0} (eV)	F_{n1} (eV)	F_{n2} (eV)	F_{n3} (eV)	F_0 (eV)	F_1 (eV)	F_2 (eV)	F_3 (eV)
Cu	0.921	−2.176	−0.140	0.286	−1.751	−2.190	0.000	0.703	0.684
Ti	0.560	−3.200	−0.200	0.680	−2.320	−3.220	0.000	0.610	−0.750

condition for invariance

$$\phi^{ab}(r) = \frac{1}{2}\left[\frac{f^{b}(r)}{f^{a}(r)}\,\phi^{aa}(r) + \frac{f^{a}(r)}{f^{b}(r)}\phi^{bb}(r)\right], \tag{10}$$

where ϕ^{ab} is the alloy potential, f is the density function as given by (4) and the superscripts aa and bb stand for monatomic a and monatomic b, respectively. The energy in the EAM model can be evaluated with about the same amount of computational work as simple pair potentials. Therefore, it is still feasible to perform large-scale computer simulations of a wide variety of phenomena. The EAM provides a powerful new technique for atomistic calculations of metallic systems with the MD simulations.

3. Simulation technique

In a general trench-filling MD simulation, one usually needs a trench model, a deposition model, and a potential model. The trench model is constructed in the form of a thin Ti film with an outer thermal control layer whose function is to keep the substrate at desired temperature. The deposition model is to characterize the incident collimation, the incidence energy, and the substrate temperature as they affect the trench-filling morphology. Lastly, suitable potential models are adopted to properly simulate the interatomic forces which exist among the trench atoms, the incident atoms and between the incident and trench atoms. Specifically, we consider the sputter deposition of copper atoms onto a trench with titanium barrier film. A schematic diagram of the trench model used in the present MD simulation is depicted in Fig. 1(a). A three-dimensional model is used to simulate the trench-filling process. The width of trench is 10.0 nm, the height is 10.0 nm, the aspect ratio (AR) is 1, and the depth of trench is 2.25 nm. Initially, the trench structure is composed of nine uniform atomic Ti layers and is divided into three layers with each layer containing three atomic layers as shown in Fig. 1(a). The outer layer is called the barrier layer, the middle layer called the thermal control layer, and the inner layer the fixed layer. The middle layer is used to control the thermal state of the barrier layer and is referred to hereafter as the"thermostated layer". Due to intrinsic limitation of MD computation, the depositing rate (the number of atoms added into the system per certain time-steps) is higher than that in practice. In order to preserve the validity of the results, we assume the energy transfer into the thermostated layer rapidly and the substrate atoms attain their thermal equilibrium rather quickly. This assumption can be realized through the velocity scaling method, which keeps the substrate at desired temperature, referred to thereafter as the "substrate temperature". Next, the barrier layer is coated with Ti

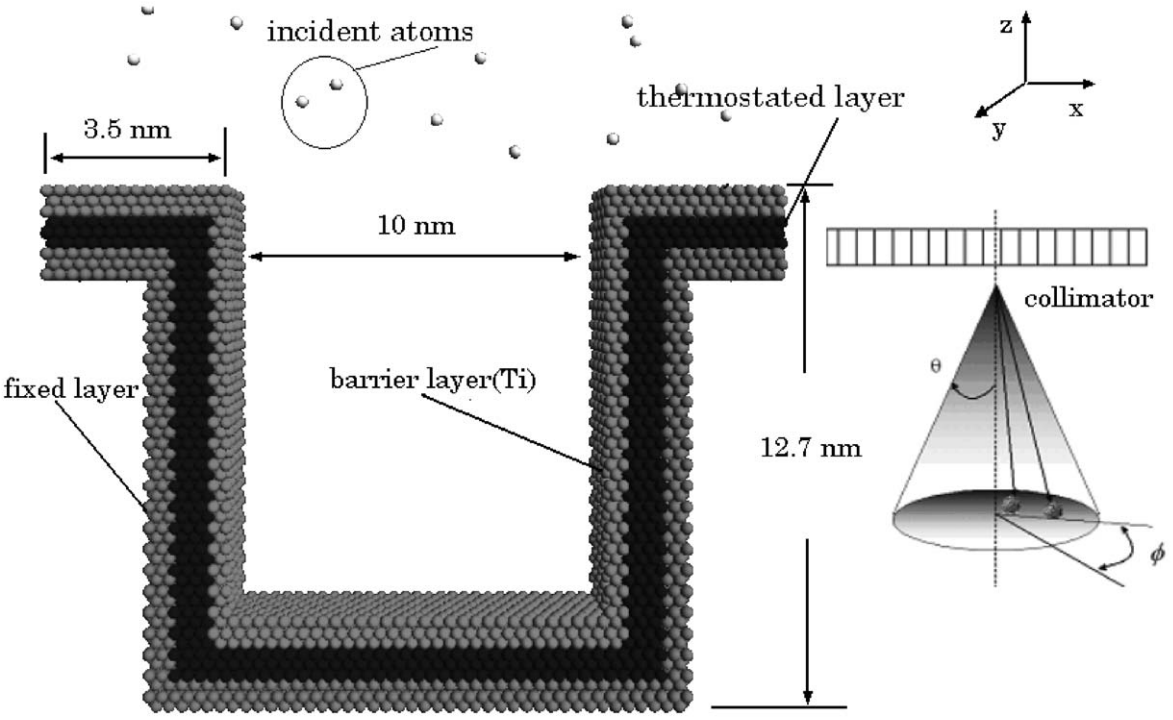

Fig. 1. (a) Schematic diagram of trench model and (b) angular distribution of incident atoms.

film on the thermostated layer. Finally, to prevent the substrate from being distorted by incident atoms during deposition, the fixed layer comprising of anchoring atoms is used. The positions of barrier layer, thermostated layer, it and fixed layer are arranged by hexagonal closed-packed (HCP) crystal structure initially with a total number of 8352 Ti atoms. The initial velocities of thermostated layer and barrier layer are given by Maxwell–Boltzmann distribution that depending on the temperature of substrate. The interactions between barrier layer and thermostated layer were relaxed before MD simulation. The positions of fixed layer atoms are frozen during simulating process and the velocities are zero before simulation. In thin films of planner structure, the thermostat layer is moving as simulation is advanced, but the trench is not of planner structure; it is difficult to find out the speed of thermostat layer to rescale the velocity of atoms. So, in this work, the thermostat atoms take the role to disperse the energy coming from incident atoms with kinetic energy. The velocities are rescaled per one time-step of simulation to keep the temperature of substrate constant. On each side of the trench opening, a trench wing is added and capped by thermal control layer and the fixed layer to absorb the impact energy produced by the bombardment of high-energy incident atoms. The inclusion of trench wings also permits the study of the influence of incident atoms impacting upon the accumulation of deposited atoms to either side of the trench opening. This can eventually affect the final morphology significantly. For incident atoms, the Cu atoms are used. The positions of the incident atoms are provided randomly in x and y directions and the magnitude of velocity is determined by $\sqrt{2E_{\text{atom}}/m}$, where E_{atom} represents the incident atom energy and m is the atomic mass. The angular distributions of collimated incident sputtered atoms are assumed to be confined within the range of zenith angle, from -5° to $+5^\circ$, and the range of azimuth angle, from 0° to 360°. The configuration of the model is shown in Fig. 1(b). To reduce the number of simulated atoms and to minimize the effects of a limited system size, periodic boundary conditions are used in x- and y-directions. The cutoff range of interaction between atoms is 6 Å which is determined by alloy potential of Cu–Ti due to the fact that the interatomic potential approaches zero near interatomic distance 6 Å. In this work we do not consider the re-deposition, i.e., the already deposited atoms Cu atom and Ti atoms on the substrate, which are moving away from the substrate during later simulation and these atoms are referred to hereafter as the "free atoms". During a deposition simulation, we detect free atoms that no longer interact with the substrate by observing force value of each atom; atoms that have zero force value during a time-step have no neighboring atoms. We label these atoms as free atoms in our program and these free atoms are removed from the system. In MD simulation, the trajectories of atoms are determined by Newton's equation of motion. After obtaining the interaction force, the phase coordinates of atoms are integrated by the Velocity–Verlet scheme [18]:

$$\mathbf{r}_i(t+\Delta t) = \mathbf{r}_i(t) + \mathbf{v}_i\left(t+\frac{\Delta t}{2}\right)\Delta t, \tag{11}$$

$$\mathbf{v}_i(t+\Delta t) = \mathbf{v}_i\left(t+\frac{\Delta t}{2}\right) + \mathbf{a}_i(t+\Delta t)\frac{\Delta t}{2}, \tag{12}$$

where $\mathbf{v}$ is the velocity vector, $\mathbf{r}$ the position vector, $\mathbf{a}$ is the acceleration vector of atom i, and Δt is time interval of simulation which is 10^{-15} s. The most severe restriction on the size of time-step Δt is due to the vibrational frequencies of the atoms [19]. For atoms in most solids, the magnitude of Δt is on the order of femtoseconds (10^{-15} s), thus, it is almost not feasible with MD simulation to observe longer term behavior such as full-scale trench-filling process over a device feature. However, interesting microscale behavior can be MD simulated that takes place within a few nanoseconds (10^{-9} s) such as the trench-filling process.

4. Result and discussion

The total number of atoms simulated in this work is on the order of 30,000 atoms. For the trench, including the atoms of barrier, thermostated and fixed layers, there are 8352 Ti atoms. For incident atoms, about 20,000 Cu atoms are used, and the depositing rate is 6 atoms per pico second (10^{-12} s). We will investigate the influences of incident energy of Cu atom and substrate temperature during trench filling on the morphology and microstructure of the trench. Three incident energies, 1, 3, and 10 eV and three substrate temperatures, 300, 425, and 550 K are considered. Finally, results are demonstrated in three-dimensional plots at various stages of deposition to help explaining and understanding the trench-filling process. Particular attention is paid to the deposition coverage along the vertical and horizontal surfaces and trench wings as they will affect the whole structure of the final morphology.

4.1. Effect of incident energy

We consider the effects of incident energy on the morphology of the trench filling by varying the incident energies and keeping the substrate temperature constant at 300 K. The first result is for the case of low incident energy, 1 eV, which is near the lowest energy of sputtering. A series of snapshots of the trench-filling morphologies are shown in Fig. 2, where the white balls are depositing Cu atoms which have not interacted with the substrate yet and the dim gray balls are deposited

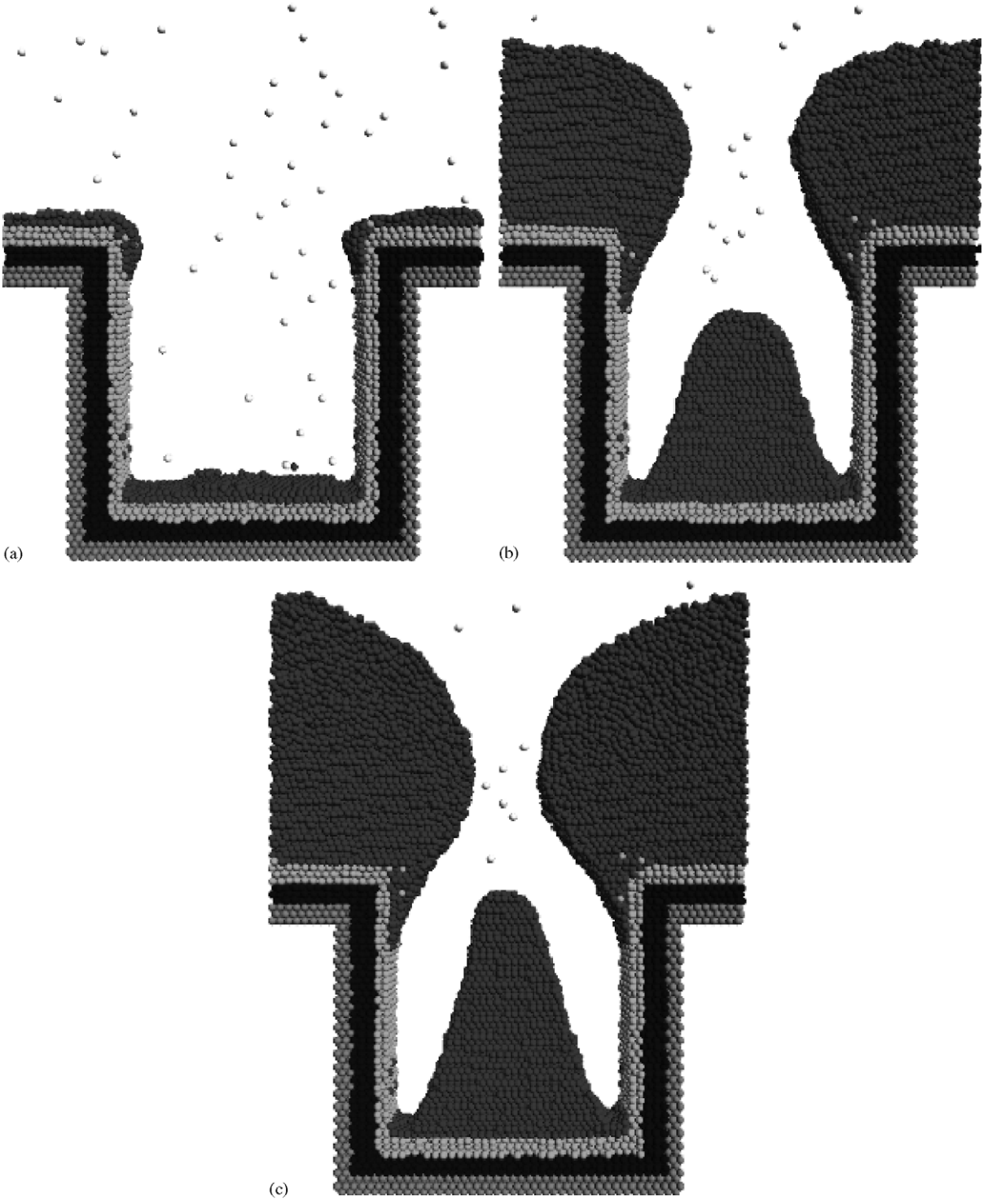

Fig. 2. Snapshots for $E_{atom} = 1\,eV$ and $T_{sub} = 300\,K$: (a) 240 ps, (b) 3020 ps and (c) 4130 ps.

Cu atoms as shown in Fig. 2(a). As time evolves, many more Cu atoms deposited on the trench wings and the height of the deposited Cu film is growing upward which is called overhanging cluster. Due to overhanging cluster, the shape of deposited atoms on the bottom looks like "hill" that the probability for Cu atoms to

pass through the gap between overhanging clusters to reach the two bottom corners is lower than that to reach the bottom center as shown in Fig. 2(b). This phenomenon is called the shadowing effect in which the overhanging clusters impede subsequent incident atoms from reaching the bottom corners. We can find that the Cu atoms will not fill the trench and two clusters on the both opening will be connected after longer-time deposition, as shown in Fig. 2(c). In the case of incident energy, 3 eV, the thickness that overhangs on the trench is thinner than that of 1 eV, due to higher incident energy bombarding the already deposited Cu clusters, and they are growing in the lateral direction and the overhanging clusters migrate further towards the base of the trench. Eventually, the two overhanging clusters grow to such a size that they touch each other and connect together and result in voids forming and become trapped within the trench, see Fig. 3(b). This phenomenon is called void formation which can affect the current flow due to the decreasing electric charges per unit cross section of trench. At the early stage of deposition, the deposition morphology on the bottom is lower but as the overhanging cluster is growing later there exists also a "hill" on the center of trench bottom. Depending on the incident energy, either the two overhanging clusters touch each other first and then meet with the center peak or sometimes the two overhanging clusters meet with the bottom peak first and then they contact each other. Both can result in the formation of voids within the trench, as shown in Fig. 3(c). However, the size of the trapped void is reduced due to the punch effect generated by the higher incident energy. At even higher incident energy, 10 eV, the morphology of the bottom becomes even more planner and the Cu clusters on the both wings of trench are slimmer as shown in Fig. 4(a). The even higher incident energy makes the punch effect more profound and flattens the bulge at bottom center meantime improves thecoverage of the two corners, as can be seen in Fig. 4(b). Also, the Cu clusters on the trench opening will merge with each other and a big void is formed first. At a later time, the "bridge" of deposited Cu atoms is bombarded by continuous incident Cu atoms then the "bridge" will merge with the bottom deposited Cu atoms, see Fig. 4(c). The void will be reduced from a big one into two smaller voids and the total void fraction is reduced. According to the above results, the void fraction can be reduced as the incident energy of Cu atoms is increased. From the cases studied above, the deposited Cu cluster on the wings of trench is thicker as the incident energy is lower and the top of the deposited Cu cluster on the bottom is more acute for low incident energy and is contrary for higher incident energy. The void fraction will be reduced that depends on the distribution of deposited atoms on the bottom and the migration of the top cluster atoms on the trench opening. Next, we investigate the intermixing of Cu and Ti atoms during the complete deposition process; alloy fraction in trench affects significantly the physical properties of the device. The interface intermixing is that the positions of Ti atoms are replaced by deposited Cu atoms on the substrate. The intermixing of Cu and Ti atoms is through an atomic exchange mechanism. This atomic exchange mechanism has been studied for vapor deposition of metal multilayers by Zhou and Wadley [20]. They found that the probability of exchange mechanism increases with the adatom energy strongly. The exchange mechanism depends upon the energy barrier at flat surface and edges of substrate and the mass of metal atoms. We can find that the intermixing will occur on the trench opening first because the total energy barrier there is less than that of other regions. Furthermore, the amount of alloy fraction becomes serious for higher incident energy of Cu atoms. As time evolves, the Ti atoms will be propagated into Cu atoms cluster. As for the microstructure of trench, the deposited Cu films are more uniform with low incident energy, i.e., the intermixing is not as serious as that with high incident energy.

4.2. Effects of substrate temperature

To investigate the effects of substrate temperature on the filling coverage of the trench and trench-filling morphology, we consider three temperatures, 300, 425, and 550 K while the incident energy is kept at 3 eV. The case of 300 K was presented and discussed before, see Fig. 3. As the substrate temperature is increased to 425 K, the height of deposited Cu film is lower on the bottom of trench and the trench wings as shown in Fig. 5(a), because of more thermal energy transfer into deposited Cu atoms from Ti thermostated layer, and the clusters are first connected as shown in Fig. 5(b) and then voids are formed after the connected clusters touched the bottom bulge, and finally, as time evolves, there are two voids formed within the trench, see Fig. 5(c). The overall morphology and microstructures for the case of 3 eV and 425 K are quite similar to that of 3 eV and 300 K except that the alloy fraction is higher for the former case. As the substrate temperature elevated to 550 K, due to the higher temperature of Ti film, the deposited Cu atoms gain additional thermal energy from the high-temperature Ti atoms and improve their mobility and become more movable when bombarded by subsequently incident Cu atoms. The deposited cluster on the side (vertical) walls with higher thermal energy will flow further downward along both the side walls and the two bottom corners are better filled, see Fig. 6(a). Due to more space available between the two trenching openings, many more Cu atoms will be deposited within the trench before the top deposited atoms on the side walls merge with bottom deposited

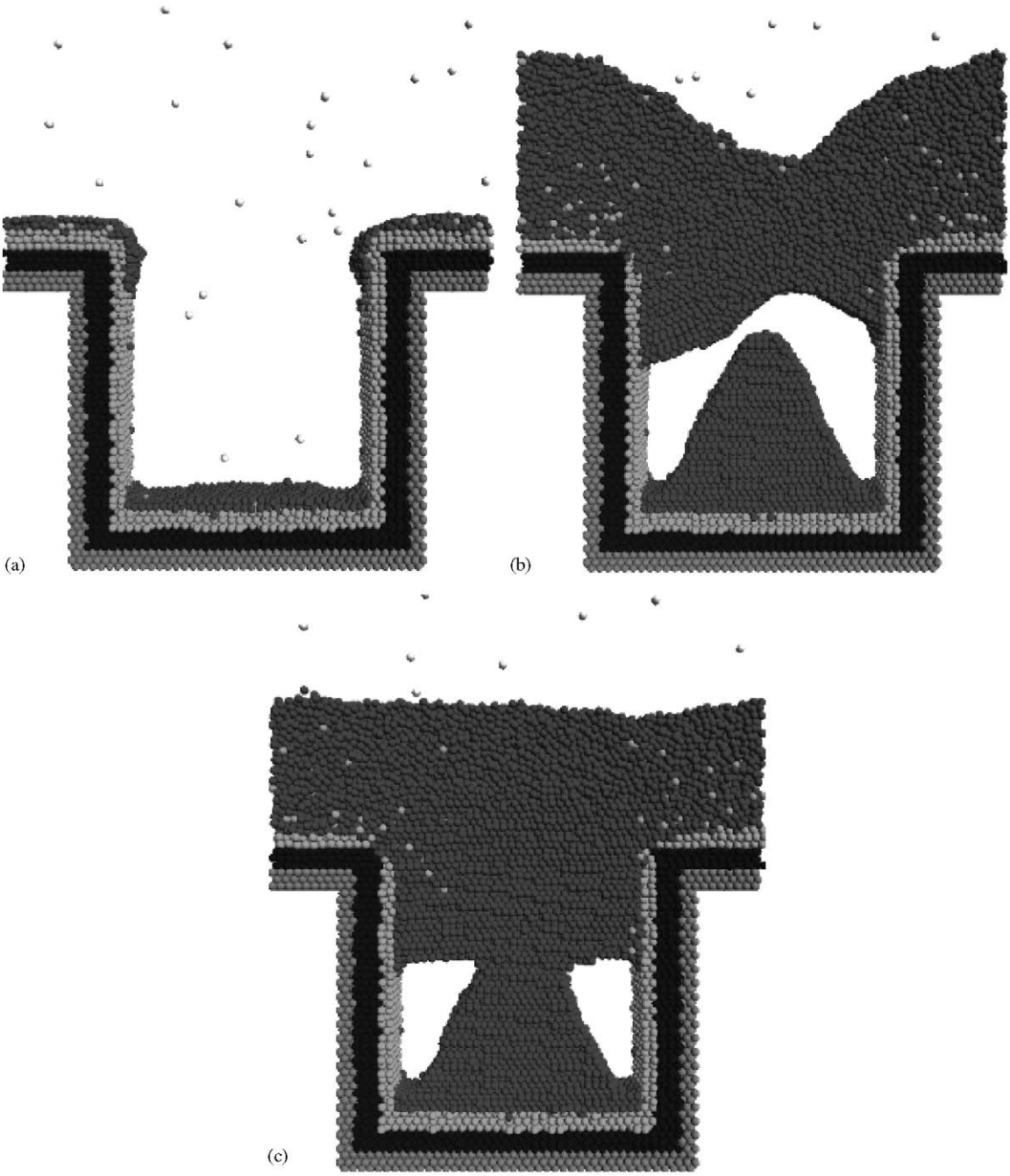

Fig. 3. Snapshots for $E_{atom} = 3\,eV$ and $T_{sub} = 300\,K$: (a) 200 ps, (b) 2160 ps and (c) 3680 ps.

atoms. Later, one of the cluster touches the bottom bulge first and a void is formed as shown in Fig. 6(b). This is different from that of 425 K case. At further later time, the other cluster touches the already merged cluster and bottom bulge and another void is formed, as shown in Fig. 6(c), and the void fraction is reduced in this case as compared with Fig. 5(c). Thus, the trench filling is promoted and the size of trapped voids is reduced by increasing the substrate temperature. This is further evidence that an elevated substrate temperature improves the fluidity of the deposited Cu atoms. The status of intermixing increases with the substrate

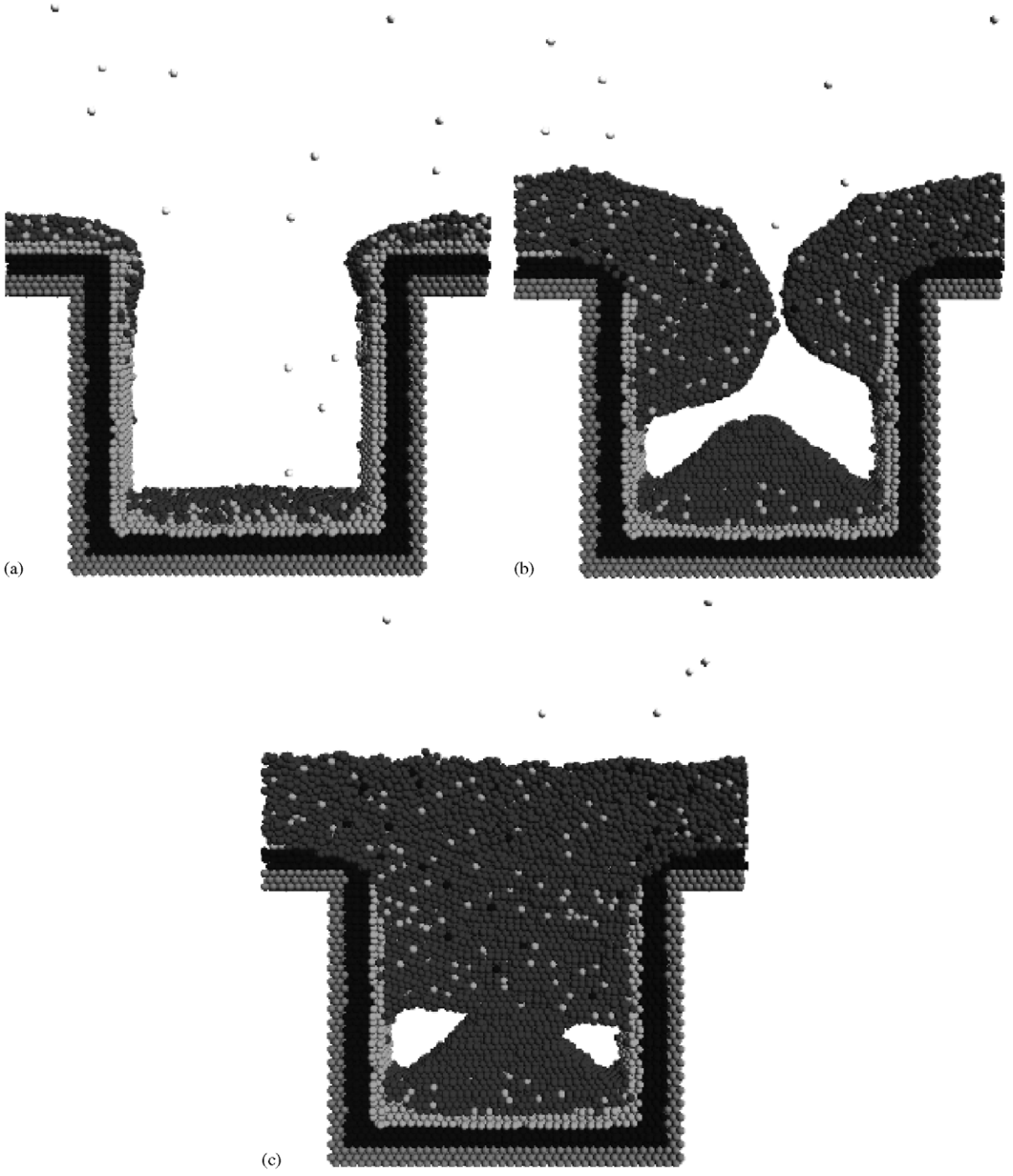

Fig. 4. Snapshots for $E_{atom} = 10\,eV$ and $T_{sub} = 300\,K$: (a) 240 ps, (b) 2200 ps and (c) 3160 ps.

temperature, because more thermal energy transfers into deposited Cu atoms from Ti thermostated layer, as those observed in the above cases of increasing incident adatom energy. The thermal energy is higher for deposited Cu atoms and Ti films, when the energy reaches the threshold of barrier energy then the exchange mechanism occurs. Although, the trench filling is promoted by increasing the substratetemperature but the accompanying effect of intermixing increase is also needed to be considered in practice. As suggested in [20],

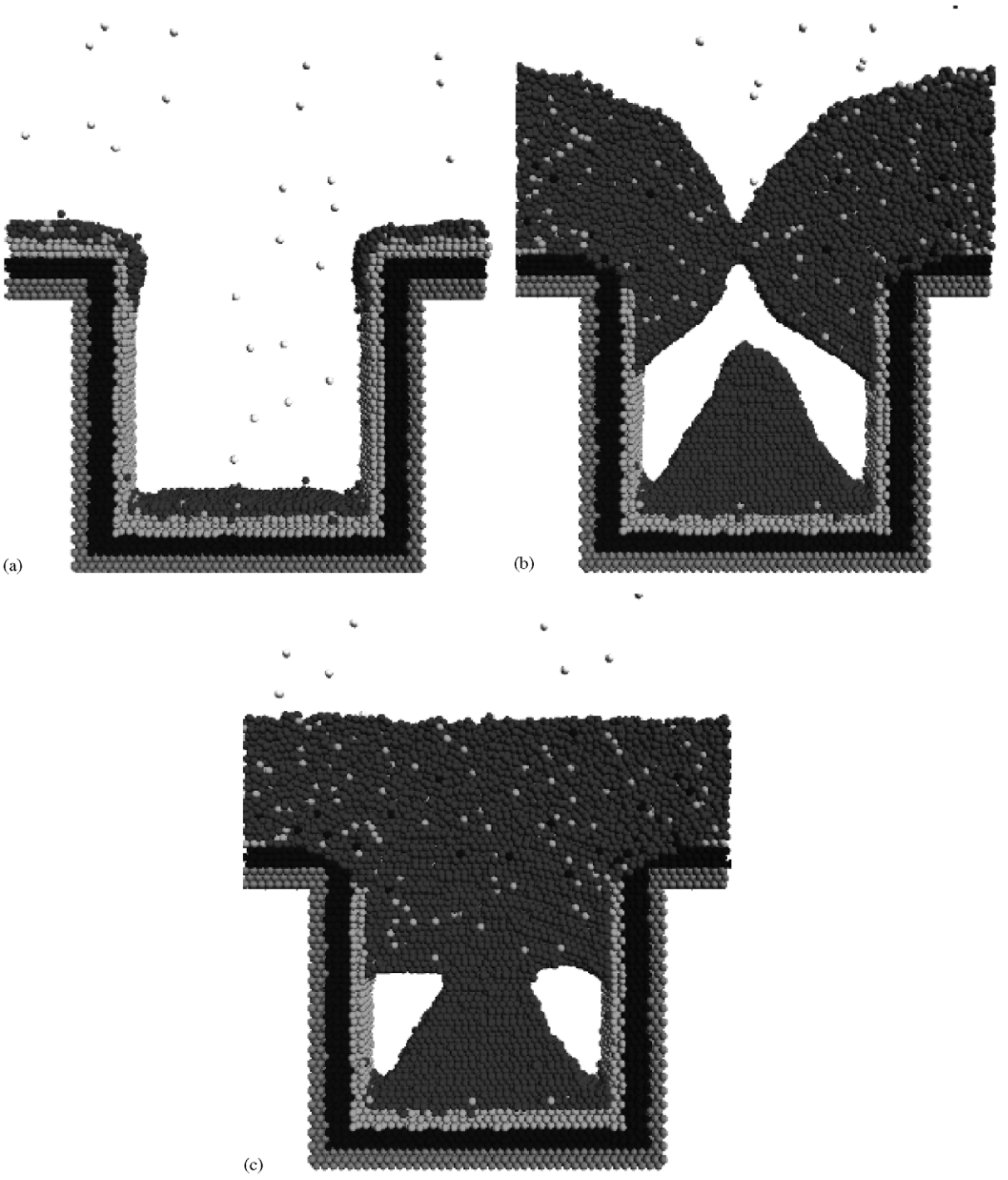

Fig. 5. Snapshots for $E_{atom} = 3\,eV$ and $T_{sub} = 425\,K$: (a) 240 ps, (b) 3280 ps and (c) 3480 ps.

the use of modulated incident atom energy deposition strategy can improve the interfacial smoothness and reduce the intermixing of Ti and Cu atoms. The coverage percentages of trench filling for various cases are shown in Fig. 7, which indicate the significant effects of the incident atoms energy (denoted by $\triangle$) and the substrate temperature (denoted by $\diamond$). The coverage percentage is determined as the number of deposited atoms within the trench divided by the number of atoms required for perfect coverage in hcp crystal structure

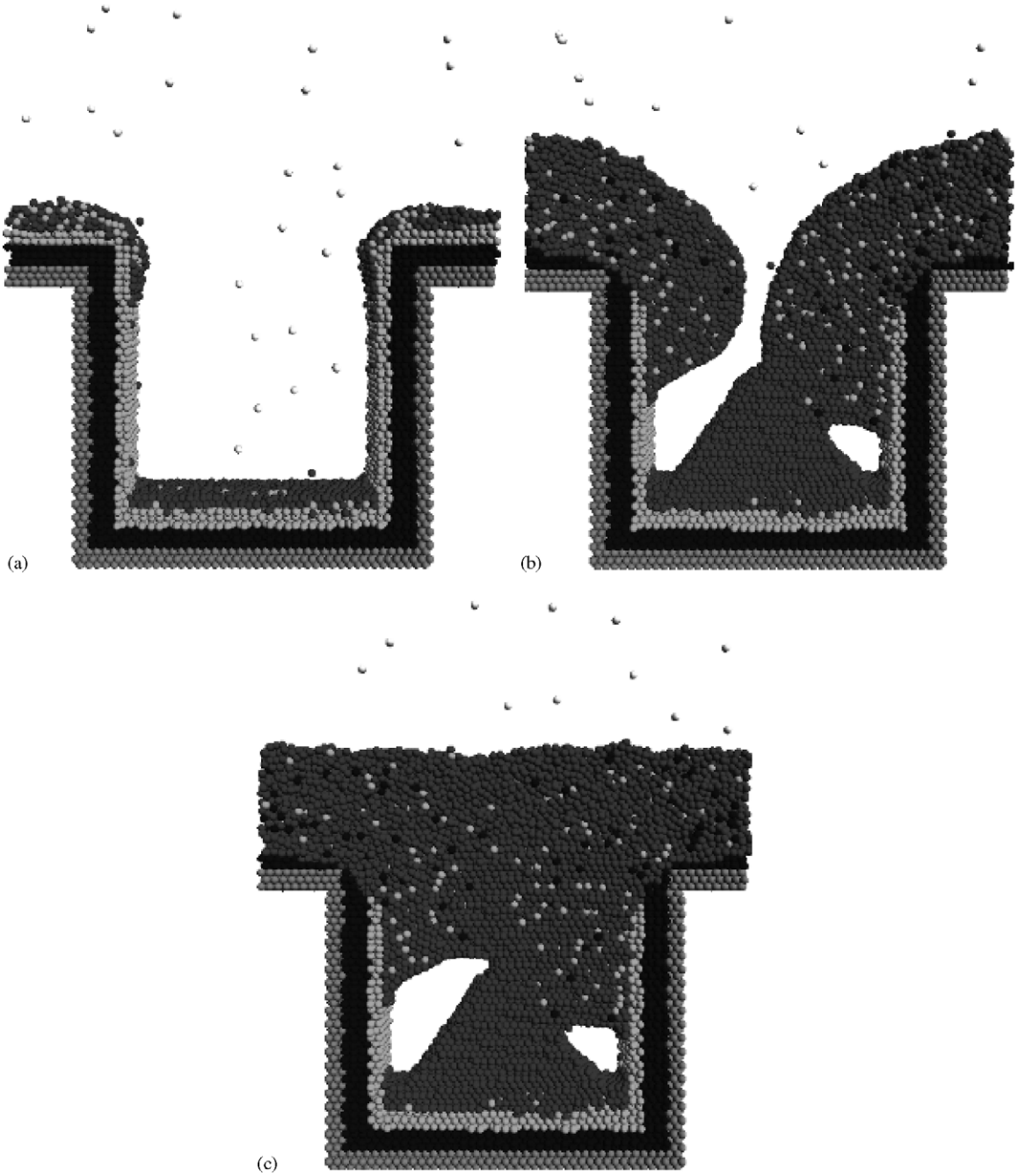

Fig. 6. Snapshots for $E_{atom} = 3\,eV$ and $T_{sub} = 550\,K$: (a) 240 ps, (b) 2560 ps and (c) 3120 ps.

within the trench. At constant 300 K substrate temperature, the coverage percentage is poor for the case of low incident energy as compared with that for higher incident energies. At constant 3 eV incident atoms energy, the coverage percentage is promoted from 80% to about 84% with temperature increase from 300 to 550 K, because with higher substrate temperature the barrier layer will be distorted rather seriously. The effect of higher substrate temperature does not improve the coverage percentage much with Ti atoms in barrier layer.

4.3. Effects of alloy model

Finally, we examine the differences of trench-filling morphologies between two different EAM models of

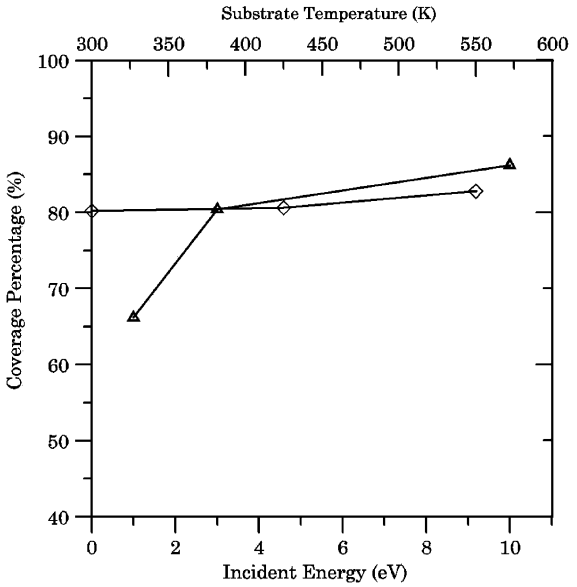

Fig. 7. A comparison of the coverage percentage for different cases. (△) is for various incident energies at constant 300 K and (◇) is for various substrate temperatures at constant 3 eV.

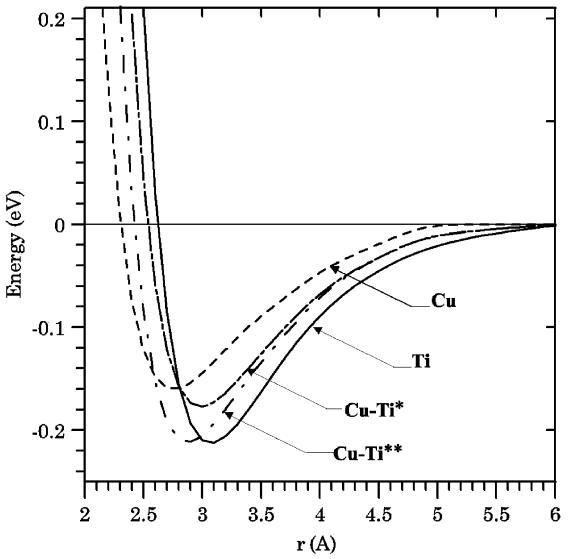

Fig. 8. The two-body potentials of copper, titanium, and their alloy. (∗) Arithmetic average (∗∗) Johnson's model.

alloy two-body potential, namely, the usual simple arithmetic average model (average model) and Johnson's invariance-preserving model (Johnson's model). In previous works about thin-film deposition simulations, the arithmetic average is most commonly used. The alloy two-body potential of average model is calculated by summing the two two-body EAM potentials of pure Cu and pure Ti and then divided by two. In Fig. 8, we plot the two alloy two-body potentials together with their individual pure element potentials. It is noted that the two potential models are nearly equal when the distance between atoms is greater than 3.5 Å. But when the distance is less than equilibrium distance that the potentials display big difference between the two models. To examine the effects of interface for two two-body potential models, the intermixing composition percentage of alloy is calculated after Cu depositing on Ti substrate. The intermixing composition percentage is computed as the ratio of the number of deposited Cu or Ti atoms divided by the total number of atoms per unit thickness of 2.54 Å (the closest distance of Ti atom in hcp crystal structure in z direction) along z direction. The substrate temperature is kept at 300 K and depositing rate is 6/ps. In Fig. 9(a), for lower incident energy 3 eV, the intermixing composition percentage displays little difference between the two models. In the case of higher incident energy, 10 eV, the thickness of intermixing is near 12 Å and the interface is cleaner for average arithmetic model but in Johnson's model the thickness of intermixing is near 28 Å which indicates that the intermixing is stronger with Johnson's model during the higher incident energy as shown in Fig. 9(b). At higher incident energies, the alloy fractions are quite different for the two models compared. Based upon the above results, we compare the microstructure of trench-filling morphology with these two models for higher incident energy 10 eV. The trench-filling morphology of average model is shown in Fig. 10. The outcome of trench filling is similar to that with Johnson's model (shown in Fig. 4) but the interfacing mixture seems to be not as serious as Johnson's except for the corner on the trench opening due to the lower barrier energy. The energy well for the Johnson's Cu–Ti model is deeper than that of simple arithmetic average model and the equilibrium distance is shorter also. That is the Cu atoms using Johnson's model have more energy when deposited into Ti substrate and cause higher temperature in the barrier layer than that using average model as shown in Fig. 11 at the early stage of deposition. Due to the higher value of diffusion coefficient ($D \propto \exp(-E/kT)$ where D is diffusion coefficient, E is the activation energy, T is barrier layer temperature, and k is the Boltzmann constant), the Cu adatoms with Johnson's model will diffuse more into the hosts atoms of barrier layer. The probability of exchange mechanism of Johnson's model is higher than that of average model. This will result in quite different deposition patterns between these two models. Comparing the alloy fraction between these two models, there are 46% of Ti barrier layer atoms mixing with deposited Cu atoms in the trench for Johnson's model while only 25% for the arithmetic average model. The present atomistic scale simulations above have indicated that high incident

energy and high substrate temperature improve trench-filling morphology but at the expense of alloy fraction increase through an exchange mechanism. One possible solution is through a modulated incident energy deposition strategy in which lower incident energy is used initially until the Cu film is formatted and then using higher incident energy to improve the coverage percentage. Although the formation of void is found existing in all the cases simulated, this shortcoming can be largely overcome by using reflow process, as suggested by typical PVD process in semiconductor manufacturing

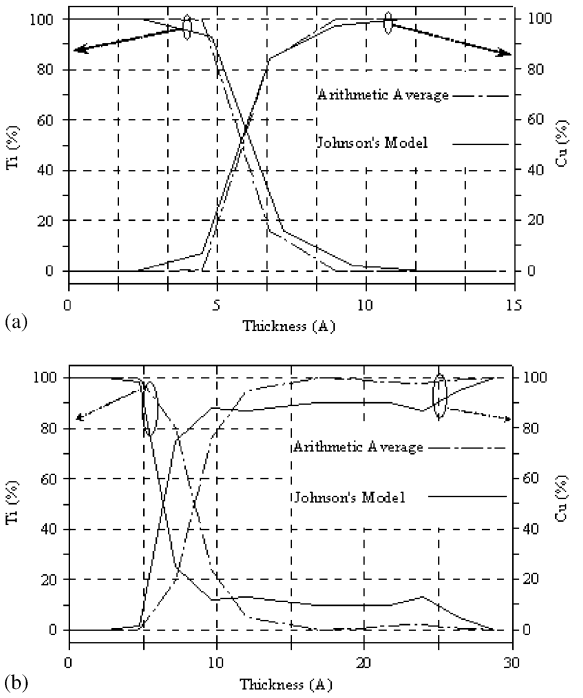

Fig. 9. The alloy composition for Cu depositing on the Ti substrate: (a) $E_{atom} = 3\,eV$ and (b) $E_{atom} = 10\,eV$.

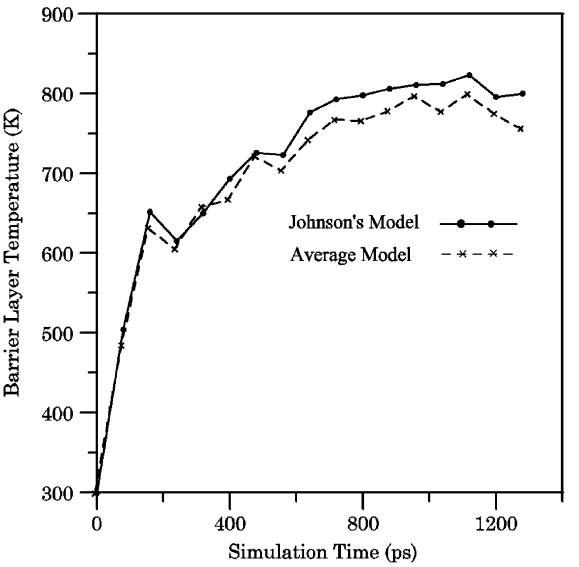

Fig. 11. The average temperature of barrier layer at early stage.

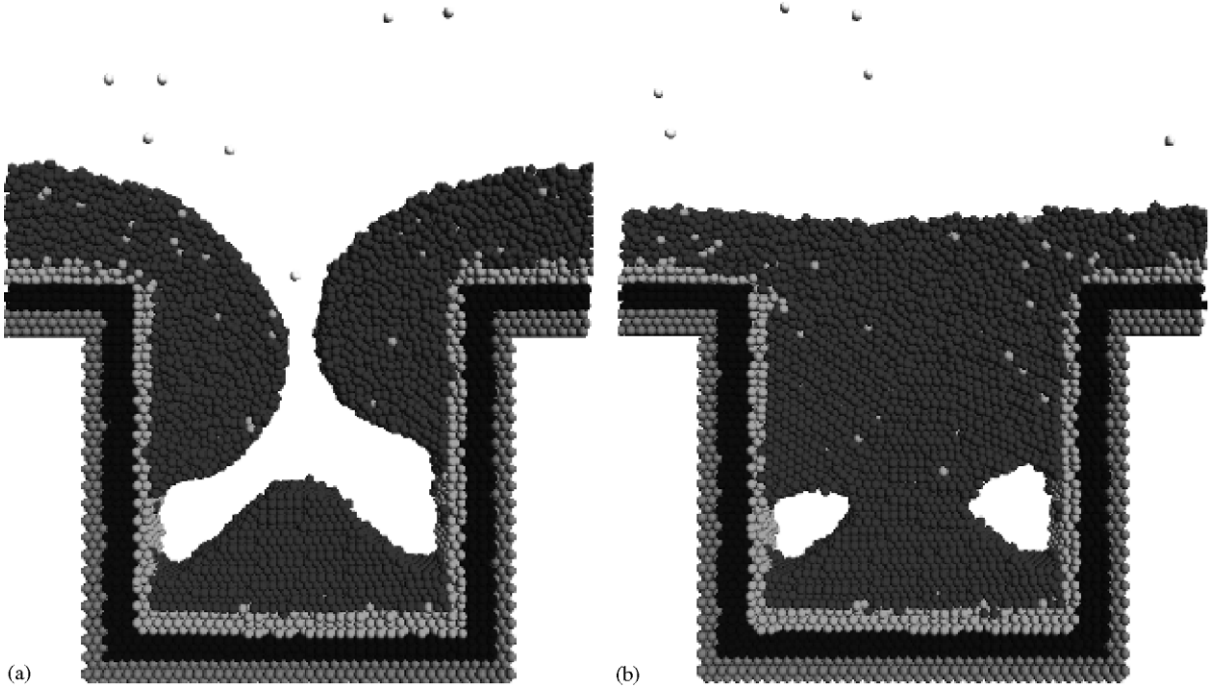

Fig. 10. Snapshots for $E_{atom} = 10\,eV$ and $T_{sub} = 300\,K$: (a) 2160 ps and (b) 2560 ps (simple arithmetic average model).

[21,22], to get better trench filling. Here, we also employ this process and the annealing temperature is set at 1000 K, and the procedure of reflow process is shown in Fig. 12. The temperature is first raised to 1000 K in 70 ps from 300 K, then it was kept at 1000 K for 210 ps and lastly it was decreased from 1000 K to 300 K in 70 ps. As time evolves, the void fraction is reduced significantly. The results after the reflow process are shown in Fig. 13 in which the smaller void can be eliminated as shown in Fig. 13(b) and the size of the bigger void reduced and the arrangement of atoms is tighter, see Fig. 13(c).

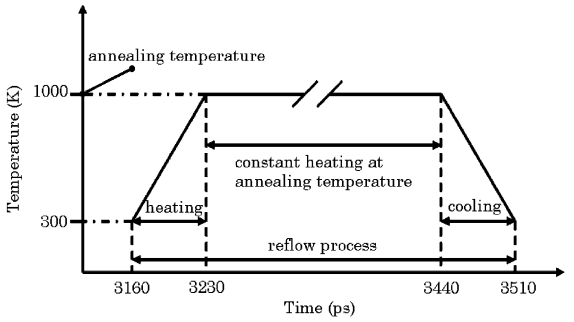

Fig. 12. Illustration of time sequence for reflow process.

5. Conclusion

The sputter deposition of copper interconnect on a titanium layer in a trench-filling process has been investigated using MD simulation in conjunction with invariance-preserving EAM interatomic potentials for the physical model. The transient behavior can be

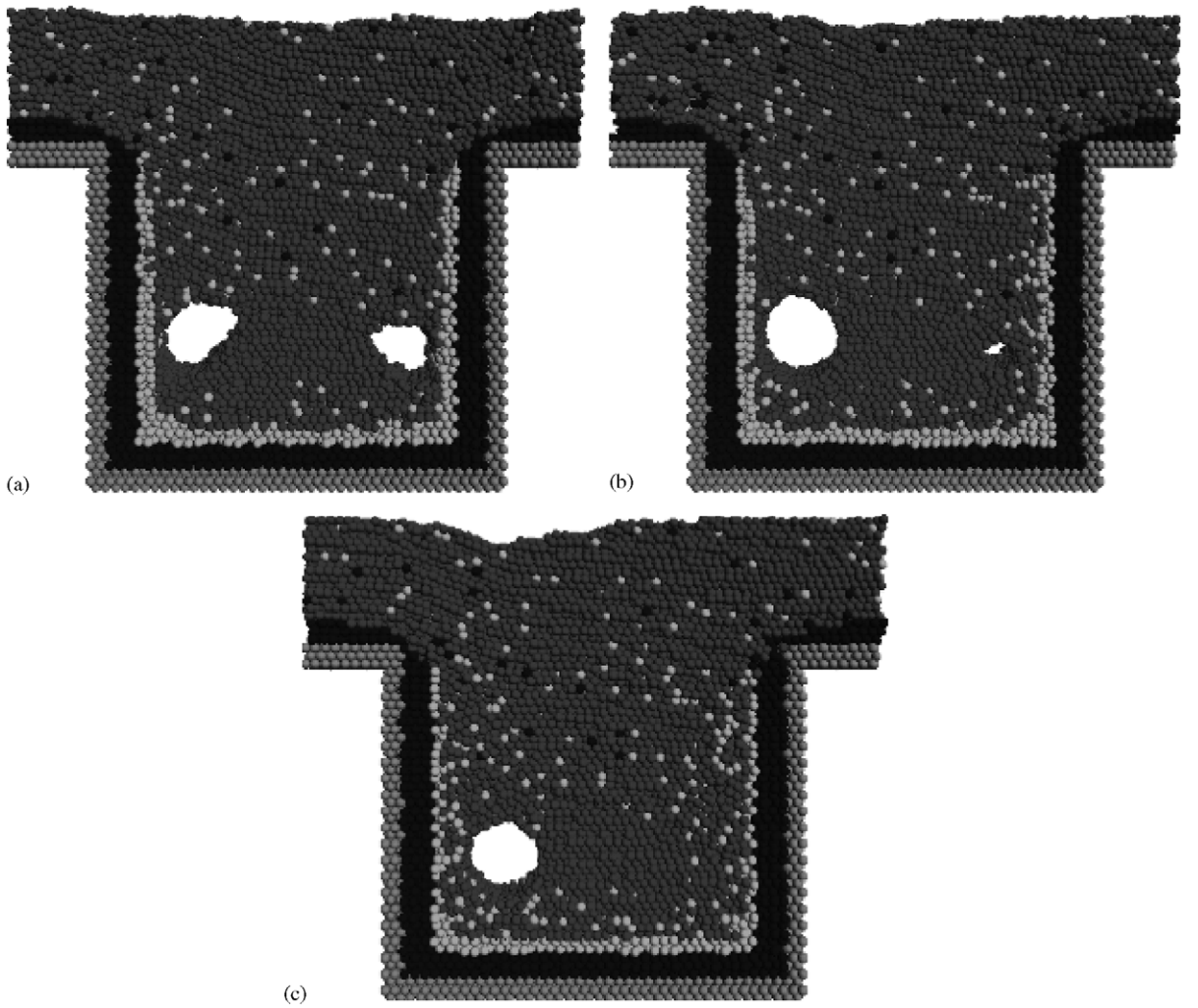

Fig. 13. The trench filling morphology with reflow process and the annealing temperature at 1000 K: (a) 3320 ps, (b) 3640 ps and (c) 4160 ps (for $E_{atom} = 10$ eV and $T_{sub} = 300$ K case).

displayed and detailed mechanism can be studied during the complete deposition process. The effects of process parameters such as incident atom energy and substrate temperature upon the morphology and microstructure are examined to provide a better understanding of this important metallization process. The key factor for a successful MD simulation depends on the use of proper potential functions that can describe the underlying physics accurately and correctly. The novel alloy model with EAM due to Johnson has been chosen for the present Cu–Ti system. Based on the present parametric study, it is possible to summarize the conclusions as following:

(i) The coverage percentage of trench filling can be promoted by increasing the energy of incident atoms and the temperature of substrate through incident atoms punch effect and increasing mobility. But the formation of Cu–Ti alloy can be significant at high incident energy and its effect on the physical properties of metal interconnect cannot be ignored. One possible solution is through modulation energy sputtering deposition in which lower incident energy is used initially until the Cu film is formatted and then higher incident energy is used to improve the coverage percentage. The interfacing mixture can also be reduced by this way.

(ii) The formation of void is dictated by step converge on trench opening and distribution of bottom deposited cluster, which is also strongly coupled with the incident atoms energy and substrate temperature. The reflow process can be implemented to effectively reduce the void fraction.

(iii) The barrier layer can be seriously distorted by higher incident energy of Cu atoms and higher temperature of substrate. It can be further studied what thickness of barrier layer is needed to avoid Cu atoms diffusing into dielectric materials in semiconductor manufacturing.

(iv) The use of simple arithmetic average alloy model can be problematic, especially when the pair distance is near equilibrium position. Johnson's invariance-preserving EAM satisfies the transformation of invariant considering the embedding energy function, potential function, and electron density function. Based on the theory, Johnson's invariance-preserving EAM alloy model is better suited for alloy systems. In damascene process, the Cu will be deposited on different types of metal barrier layer such as Ti or Ta layer and the alloy two-body potential functions need to be more realistically described, and the Johnson model can give better explanation of the intermixing of two metals during the trench-filling deposition process.

Acknowledgements

This work was done under the auspices of National Science Council, TAIWAN through Grants NSC 90-2210-E002-039 and 91-2210-E002-035. The authors would like to thank Dr S.S. Lee of tsmc for many fruitful discussions on damascene process.

References

[1] Sze M. Semiconductor devices physics and technology, 2nd ed. New York: Wiley; 2001.
[2] Hau-Riege CS. Microel Reliab 2004;44(2):195–205.
[3] Takewaki T, Ohmi T. Tech Dig Symp VLSI Technol 1995; 31–32.
[4] Hamaguchi S, Rossnagel M. J Vac Sci Technol B 1995; 13(2):183–91.
[5] Adalsteinsson D, Sethian JA. J Comp Phys 1995; 120(1):348–66.
[6] Huang CH, Glimer GH, Rubia TD. J Appl Phys 1998; 84(7):3636–49.
[7] Yang YG, Zhou XW, Johnson RA. J Vac Sci Technol B 2002;20(2):622–30.
[8] Zhou XW, Johnson RA, Wadley HNG. Acta Materialia 1997;45(4):1513–24.
[9] Ju SP, Weng CI, Su MH, Chang JG, Huang CC. J Vac Sci Technol B 2002;20(3):946–55.
[10] Stott MJ, Zaremba JE. Phys Rev B 1980;22(4):1564–83.
[11] Daw MS, Baskes MI. Phys Rev Lett 1983;50(17):1285–8.
[12] Daw MS, Baskes MI. Phys Rev B 1984;29(13):6443–53.
[13] Johnson RA. Phys Rev B 1988;37(8):3924–31.
[14] Oh DJ, Johnson RA. J Mat Res 1988;3(3):417–78.
[15] Wadley HNG, Zhou X, Johnson RA, Neurock M. Prog Mat Sci 2001;46(3–4):329–77.
[16] Foiles MS, Baskes MI, Daw MS. Phys Rev B 1986; 33(12):7983–91.
[17] Johnson RA. Phys Rev B 1989;39(17):12554–99.
[18] Verlet L. Phys Rev 1967;159(1):98–103.
[19] Rapaport DC. The art of molecular dynamics simulation. New York: Cambridge University Press; 1996.
[20] Zhou XW, Wadley HNG. J Appl Phys 1998;84(4): 2301–15.
[21] Saito Y, Hirasawa S, Saito T, Nezu H, Yamaguchi H, Owada N. IEEE Trans Semi Manuf 1997;10(1):131–6.
[22] Su MH, Huang CC, Chang JG, Ju SP. J Vac Sci Technol B 2002;20(5):1853–65.